Available online at www.sciencedirect.com
ScienceDirect
Polymer 48 (2007) 5581–5589
polymer
www.elsevier.com/locate/polymer

Physical properties of poly(cyclohexyl methacrylate)-*b*-poly(*iso*-butyl acrylate)-*b*-poly(cyclohexyl methacrylate) triblock copolymers synthesized by controlled radical polymerization

Alexandra Muñoz-Bonilla, María L. Cerrada*, Marta Fernández-García

Instituto de Ciencia y Tecnología de Polímeros (CSIC), C/Juan de la Cierva 3, 28006 Madrid, Spain

Received 3 April 2007; received in revised form 7 May 2007; accepted 20 July 2007
Available online 29 July 2007

Abstract

The microphase segregation of different poly(cyclohexyl methacrylate)-*b*-poly(*iso*-butyl acrylate)-*b*-poly(cyclohexyl methacrylate), PCH-*b*-P*i*BA-*b*-PCH, triblock copolymers obtained by atom transfer radical polymerization has been evaluated by dynamic mechanical thermal analysis through location of the two relaxations ascribed to cooperative motions of each block. Additionally, other secondary relaxations have been found, whose characteristics are also dependent on molecular weight of outer and rigid segments. The length of these hard blocks influences significantly the stiffness and microhardness found in these triblock copolymers. These two mechanical parameters increase as molecular weight of poly(cyclohexyl methacrylate) does. The morphological aspects have been examined by small angle X-ray scattering and atomic force microscopy.

Keywords: Viscoelastic relaxation; Phase separation; Triblock copolymers

1. Introduction

Controlled radical polymerization has attracted much attention over the past decade for providing simple and robust routes to the synthesis of well-defined and low polydispersity polymers. Among them, atom transfer radical polymerization (ATRP) [1–3] is one of the most widely used controlled free radical polymerization technique. This method has been applied to prepare block copolymers with well-controlled molecular weights and well-defined structures [4].

Block copolymers can be commonly induced or spontaneously self-assembled into a diversity of mesophases (spheres, cylinders, lamellae, etc.). These mesophase morphology and microdomain dimensions can be analyzed by temperature-variable real-time small angle X-ray scattering (SAXS) experiments. Moreover, block copolymers are suitable materials for many commercial applications because they allow obtaining a broad spectrum of polymeric materials combining different monomers and their respective properties. These important applications include their use as thermoplastic elastomers, and compatibilizers in polymer blends [5–7]. Recently, a more advanced applicability is being developed for these self-assembled polymeric materials. This consists of using ordered block copolymers as templates for the production of nanostructures, in nanoscale lithography, and as selectively permeable membranes in new fuel cell designs [8–11].

On the other hand, block copolymers based on acrylates and methacrylates are synthetically very interesting because of their inherent morphological, phase, and mechanical characteristics. These properties are due partly to the combination of a high glass transition temperature (T_g) associated with the rigid block (methacrylate) and another lower T_g ascribed to the much softer block (acrylate). Many of these systems have been synthesized by controlled radical polymerization [4,12–33]. However, thorough studies on mechanical properties in the

* Corresponding author. Tel.: +34 91 5622900; fax: +34 91 5644853.
E-mail address: mlcerrada@ictp.csic.es (M.L. Cerrada).

0032-3861/$ - see front matter © 2007 Elsevier Ltd. All rights reserved.
doi:10.1016/j.polymer.2007.07.056

solid state of the resultant copolymers are scarce in the literature [23,34]. The synthesis of PCH-*b*-P*i*BA-*b*-PCH triblock copolymers obtained by ATRP together with their molecular and thermal characterization has been reported in a previous work [33]. The analysis of differential scanning calorimetry, DSC, results showed that only copolymers obtained using the P*i*BA macroinitiator with the highest molecular weight clearly exhibited two glass transition temperatures and, therefore, microphase separation between blocks. This article, based on these features, aims to comprehensively study the viscoelastic response of these PCH-*b*-P*i*BA-*b*-PCH triblock copolymers by means of dynamic mechanical thermal analysis and microhardness measurements. Additionally, the microphase arrangement of outer and inner blocks is examined by real-time small angle X-ray scattering experiments and atomic force microscopy for a deep understanding of the mechanical behavior underlying and exhibited by these PCH-*b*-P*i*BA-*b*-PCH triblock copolymers.

2. Experimental

2.1. Sample preparation

Films by compression molding of these PCH-*b*-P*i*BA-*b*-PCH copolymers, for DMTA and microhardness measurements, were prepared at a pressure of 15 bar for 5 min in a Collin Press (Model 3912) between hot plates at 180 °C.

Copolymer films were prepared by casting from 8% (w/v) toluene solution for SAXS measurements. In addition, for AFM measurements, the copolymer films were prepared by spin-coating from toluene solutions (5 mg ml^{-1}) supported in mica. To further promote the formation of equilibrium morphologies, the bulk films were annealed under vacuum at 130 °C during 72 h. The films were then cooled slowly to room temperature.

2.2. Dynamic mechanical thermal analysis

Viscoelastic properties were measured with a Polymer Laboratories MK II dynamic mechanical thermal analyzer working in the tensile mode. The complex modulus and the loss tangent (tan δ) of each sample were determined at 1, 3, 10 and 30 Hz over a temperature range from −150 to 150 °C, at a heating rate of 1.5 °C/min. The specimens used were rectangular strips of about 3.5 mm wide, around 0.45 mm thick and over 16 mm long. The apparent activation energy values were calculated according to Arrhenius-type equation, employing an accuracy of ±1 °C in the temperature assignment of E'' maxima. The frequency dependence with temperature of relaxations associated with the glass transitions has also been considered to follow an Arrhenius behavior although they are ascribed to cooperative motions [35]. This approximation can be made without a significant error, since the range of analyzed frequencies is short enough to be fitted to such a linear behavior as just mentioned.

2.3. Microhardness measurements

A Vickers indenter attached to a Leitz microhardness tester was used to perform microindentation measurements undertaken at 23 °C. A contact load of 9.8 N and a contact time of 25 s were employed. Microhardness (MH) values (in MPa) were calculated according to equation [36]:

$$\mathrm{MH} = 2\sin 68^\circ P/d^2$$

where P (in N) is the contact load and d (in mm) is the length of the projected indentation area.

2.4. X-ray scattering

The morphologies developed by the copolymers with different molecular weight are followed by simultaneous time-resolved SAXS measurements using X-ray synchrotron radiation in the soft-condensed matter beamline A2 at HASYLAB (DESY, Hamburg, Germany). The experimental setup includes a heating specimen holder and a MARCCD detector for acquiring two-dimensional SAXS patterns (sample-to-detector distance being 260 cm). The different diffraction patterns represented were extracted from the all integrated SAXS profiles. In addition, WAXS profiles were recorded using a linear detector at a sample-to-detector distance of around 21 cm to estimate the existence of microphase separation. All experiments comprised the heating of initially amorphous sample from 30 up to 190 °C followed by a further cooling run at 10 °C/min, during which simultaneous SAXS and WAXS experiments were performed. The acquisition of data was done in frames of 30 s.

2.5. Atomic force microscopy

The surface morphology of the thin films was observed by a tapping mode AFM (Multimode Nanoscope IVa, digital instrument/Veeco) at ambient conditions. In tapping mode, the stylus oscillates, touching the sample only at the end of its downward movement. The nominal resonance frequency for tapping mode was between 265 and 309 kHz with phosphorous (n) doped Si cantilever which had a spring constant between 20 and 80 N/m. The set point in the AFM control program was adjusted to change the contact force between tip and surface in order to detect the existence of morphologies.

3. Results and discussion

3.1. Viscoelastic and mechanical responses

The PCH-*b*-P*i*BA-*b*-PCH triblock copolymers under study were previously synthesized by atom transfer radical polymerization in a sequential manner [33] using a poly(*iso*-butyl acrylate) macroinitiator with a molecular weight of 45.660 g/mol and $M_n/M_w = 1.12$. Their thermal analysis by DSC revealed the existence of microphase separation between the two

blocks, as previously commented. Therefore, the T_g locations of soft and hard segments, determined from calorimetric curves, were very similar to those observed in the individual blocks of analogous characteristics. In addition, this thermal behavior pointed out the completely amorphous nature of these copolymers. Accordingly, the corresponding WAXS profiles that they exhibit consist on a single amorphous halo with absence of other diffraction peaks, as seen in Fig. 1a. In spite of the relative simplicity of WAXS region, a detailed assessment of variation with temperature of the amorphous halo peak, whose position in the maximum (d^{halo}) is directly ascribed to the most probable intermolecular distance between macromolecular chains [37], can also provide information on the existence of microphase separation in these ABA copolymers. However, in these particular PCH-*b*-P*i*BA-*b*-PCH triblock copolymers, it has to be taken into account that the T_g of the inner block is found at subambient temperatures, impossible to be reached through the setup used for these diffraction experiments. Accordingly, from 20 °C – the lowest accessible temperature and above the T_g of inner segments – to around 105 °C, the location of amorphous halo maximum varies in a lesser extension than at temperatures higher than 105 °C, as depicted in Fig. 1b for PCH_{299}-*b*-P*i*BA_{355}-*b*-PCH_{299}. This fact is due to the reduced motion capability within this temperature range of the rigid PCH blocks, since these outer segments are below their corresponding glass transition temperature being, consequently, in their glassy state. Once, the whole block copolymer gains mobility at temperatures higher than about 105 °C, the position of the most probable intermolecular distance between macromolecules undergoes a significant shift to higher d^{halo} values in the same way that the d^{halo} thermal expansion coefficient increases. These features are ascribed to the existence of cooperative and generalized motions within macromolecules because of their global elastomeric state at those high temperatures. Accordingly, the glass transition temperature of the outer and rigid blocks can be estimated from the intersections of these two different slopes – fit to straight lines are represented in Fig. 1b – associated with the change of thermal expansion coefficients and, thus, to the variation of the copolymer mobility. The agreement with those T_g values obtained by DSC [33] for the outer blocks is extremely good, the calorimetric value being 106 °C for the copolymer shown in Fig. 1.

Dynamic mechanical thermal analysis (DMTA) is another useful and extended tool for T_g determination in polymers. DMTA, sometimes, exhibits even a better sensibility regarding DSC measurements. In addition, the evaluation of the viscoelastic behavior over a wide temperature scale allows knowledge on the relaxation processes that can take place in a polymer and that govern its overall mechanical response. When a polymer reaches the temperature range in DMTA experiments at which a chain movement occurs, either that one related to the generalized glass transition or also those local movements not detected by other techniques, the energy dissipated increases up to a maximum. Therefore, information on the dynamics of the polymer in the solid state can be obtained from the study of the loss magnitudes, loss modulus (E'') and loss tangent (tan δ). Moreover, the analysis of storage modulus (E'), ascribed to the part of energy absorbed into the polymer, provides a direct estimation about the stiffness along the whole temperature interval.

On the other hand, the viscoelastic response in the solid state of block copolymers is primarily determined by the mutual miscibility of the different blocks [38] and by the corresponding response of each existing block. Fig. 2 shows storage, E', and loss moduli, E'', as well as loss tangent, tan δ, for the PCH_{105}-*b*-P*i*BA_{355}-*b*-PCH_{105} triblock copolymer at the different frequencies analyzed: 1, 3, 10 and 30 Hz. Five different relaxation processes are observed in the loss representations, labeled as γ^{PiBA}, γ^{PCH}, α^{PiBA}, β^{PCH} and α^{PCH} in order of increasing temperatures. At the lowest experimental temperatures, the side of high temperature of the γ^{PiBA} relaxation is seen. Although there is, to the best of our knowledge, none study in the literature on the poly(*iso*-butyl acrylate), P*i*BA, rheological behavior, the discussion referred to its relaxation mechanisms can be based on the response of poly(*iso*-butyl methacrylate) [39] as well as that exhibited by other reported alkyl acrylates [35,40,41]. This γ^{PiBA} relaxation is

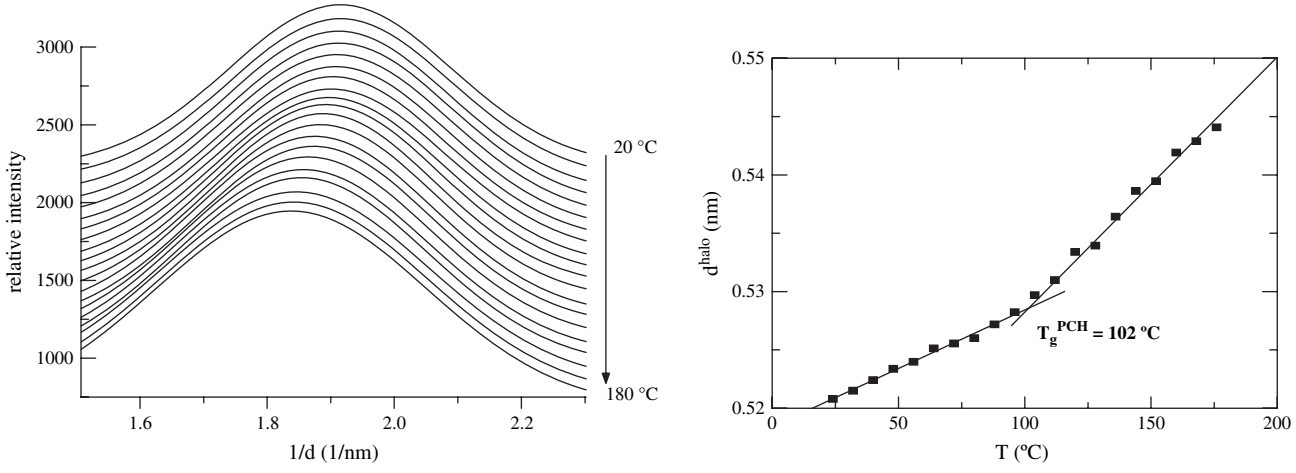

Fig. 1. (a) Time-resolved WAXS profiles for PCH_{299}-*b*-P*i*BA_{355}-*b*-PCH_{299} triblock copolymer during the heating process and (b) dependence of d^{halo} on temperature.

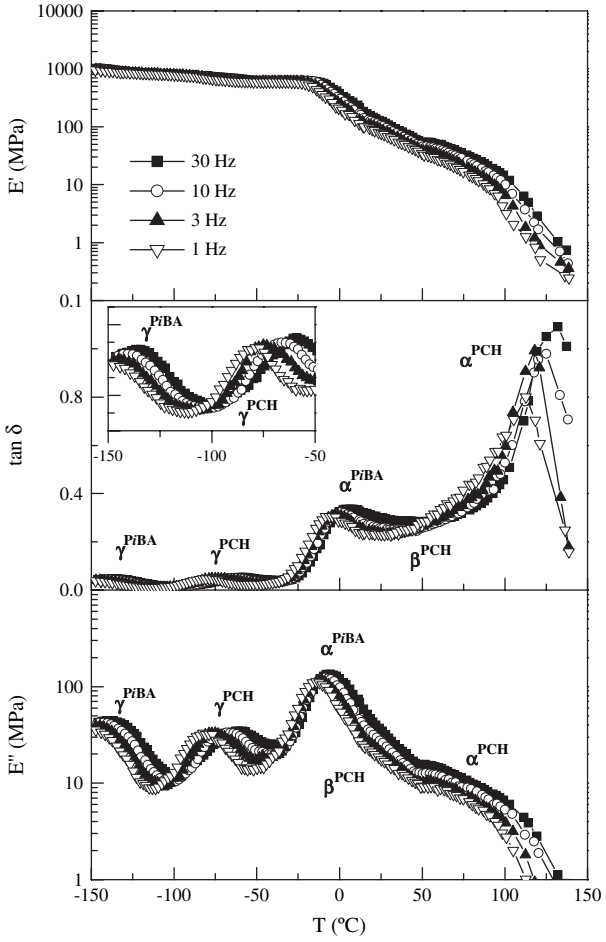

Fig. 2. Temperature dependence of the two components to the complex modulus and of the loss tangent for the PCH_{105}-*b*-P*i*BA_{355}-*b*-PCH_{105} copolymer.

molecularly ascribed to the rotation around the oxygen–*iso*-butyl bond. This process is independent of that owed to the whole oxycarbonyl group and the main chain and its location has been found strongly dependent on length and nature of the alkyl group [35]. Therefore, the γ^{PiBA} in the copolymer PCH_{105}-*b*-$PiBA_{355}$-*b*-PCH_{105} occurs at higher temperatures than that found in (meth)acrylate copolymers with *n*-butyl groups [40] in the side chains and at lower temperatures to those copolymers with *tert*-butyl pendant groups [41], i.e. $\gamma^{PnBA} < \gamma^{PiBA} < \gamma^{PtBA}$. The apparent activation energy estimated leads to a value of 40 kJ mol^{-1} that agrees to that found in the poly(*iso*-butyl methacrylate) [39]. At higher temperatures, the γ^{PCH} process takes place. It is of similar intensity to the γ^{PiBA} relaxation in this copolymer and appears at around −75 °C. The motions underlying this mechanism are now associated with the poly(cyclohexyl methacrylate) blocks [35]. This process has been primarily associated to the chair-to-chair inverse conformational transitions within the cyclohexyl ring in which the equatorial positions are exchanged with the axial ones [35]. However, molecular dynamic studies [42,43] have shown that the relaxational activity in the spectra of the poly(cyclohexyl methacrylate) and other cyclohexyl-based polymers cannot be exclusively attributed to these chair-to-chair conformational transitions. Its apparent activation energy is around 55 kJ mol^{-1} that agrees with the values found for this relaxation in other polymers [42,43].

Another much more intense relaxation, α^{PiBA}, appears at about −10 °C (see Fig. 2), depending on whether E'' or tan δ is the considered magnitude for its determination. This process is associated with cooperative motions within the soft and inner P*i*BA segments. The apparent activation energy found is much higher than that exhibited by the γ^{PiBA} and γ^{PCH} processes (see Table 1) due to the generalized motions of long chain segments that this relaxation implies. At higher temperatures, a shoulder completely merged with the α^{PiBA} and with the relaxation ascribed to cooperative motions within the PCH blocks, α^{PCH} process, is seen in the E'' representation. This completely overlapped mechanism is attributed to the β^{PCH} relaxation [35] and seems to appear at around 30–35 °C in agreement with values in the literature. Its molecular cause is related to movements that imply the whole lateral CO–*O*-cyclohexyl groups. This β relaxation in other methacrylates, as for instance poly(methylmethacrylate), PMMA, is characterized by its intensity and the broadness of its relaxation time distribution. However, this mechanism in the PCH is not as intense as that in PMMA most likely due to the great rigidity of the cyclohexyl group [44,45] compared to that of the methyl group. Its location between the two main relaxation processes of both inner and soft segments and outer and hard blocks within this copolymer PCH_{105}-*b*-P*i*BA_{355}-*b*-PCH_{105}, α^{PiBA} and α^{PCH}, respectively, is responsible of its complete overlapping. An accurate determination of its maximum and, therefore, the estimation of its apparent activation energy are impossible.

However, these loss moduli curves in these PCH_X-*b*-P*i*BA_{355}-*b*-PCH_X copolymers under study are well described as composed by contribution of different Gaussian curves, one for each observed relaxation process. Such a convolution does not have a theoretical basis that can explain satisfactorily the shape of the dependence of loss modulus on temperature, though some factors that can influence it are known. A method of curve convolution to analyze the dynamic mechanical loss curves in the region of the glass transition of several polymers has been proposed [46] confirming the validity of this empirical approximation. In addition, it was shown that a Gaussian function provided the best fitting. In the present case, the summation of five Gaussian curves for PCH_X-*b*-P*i*BA_{355}-*b*-PCH_X copolymers yields a very good overall fitting over the whole experimental range measured, as seen in Fig. 3 for E'' in PCH_{105}-*b*-P*i*BA_{355}-*b*-PCH_{105}. This convolution is a very useful tool for the assessment of different relaxation location

Table 1
Characteristics of PCH_X-*b*-P*i*BA_{355}-*b*-PCH_X triblock copolymers

Sample	PCH M_n (SEC)	CH content (^{1}H NMR)	M_w/M_n	D^{SAXS} (nm)
PCH_{105}-*b*-P*i*BA_{355}-*b*-PCH_{105}	8400	0.37_2	1.50	–
PCH_{219}-*b*-P*i*BA_{355}-*b*-PCH_{219}	39,300	0.55_2	1.28	38
PCH_{299}-*b*-P*i*BA_{355}-*b*-PCH_{299}	53,300	0.62_7	1.30	40
PCH_{380}-*b*-P*i*BA_{355}-*b*-PCH_{380}	70,400	0.66_9	1.26	42

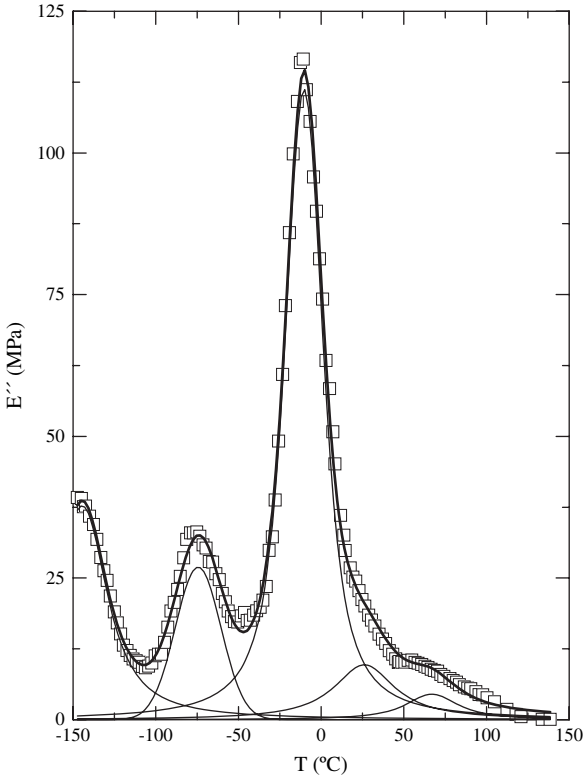

Fig. 3. Deconvolution of PCH_{105}-*b*-P*i*BA_{355}-*b*-PCH_{105} loss modulus curve at 3 Hz (symbols) into five relaxation processes (thin lines) and the overall fit (thick line).

when overlapping of processes is important. Accordingly, data listed in Table 2, related to the temperature location of the different relaxations, are taken from E'' plots after their corresponding deconvolution.

Concerning the variation of E' values with temperature, these do not change too much with frequency up to approximately −25 °C due to the existence of only secondary relaxation processes below that temperature (see Fig. 2). Therefore, storage modulus drops steadily until this commented temperature mostly because of the existence of the two mentioned secondary processes, γ^{PiBA} and γ^{PCH} and the thermal expansion [47]. However, a more clear dependence with frequency is exhibited at temperatures higher than −25 °C due to the proximity to the glass transition temperature of the inner and soft P*i*BA blocks and even more significant variation with frequency is seen in the immediacy of the cooperative motions within the stiffer outer segments of poly(cyclohexyl methacrylate).

Fig. 4 shows the effect of composition on the loss magnitudes, E'' and tan δ, for the different PCH_X-*b*-P*i*BA_{355}-*b*-PCH_X copolymers. The intensity dependence of the different relaxation processes on outer blocks molecular weight is clearly seen looking at the tan δ plot. This magnitude is rather sensitive because of its independence of E' values during measurements. Therefore, the variation of intensity for the γ^{PiBA} relaxation is PCH_{105}-*b*-P*i*BA_{355}-*b*-PCH_{105} > PCH_{219}-*b*-P*i*BA_{355}-*b*-PCH_{219} > PCH_{299}-*b*-P*i*BA_{355}-*b*-PCH_{299} ≈ PCH_{380}-*b*-P*i*BA_{355}-*b*-PCH_{380}, i.e. intensity decreases as relative P*i*BA composition in the copolymer does because of its molecular origin. It seems that once a determined molecular weight is exceeded, γ^{PiBA} intensity remains almost constant. Independent of length in the outer blocks, it can be said that this relaxation appears at around −148 °C for all of the copolymers PCH_X-*b*-P*i*BA_{355}-*b*-PCH_X and its apparent activation energy is 40 kJ mol^{-1}.

The opposite trend for the intensity of γ^{PCH} mechanism is observed, as depicted the inset in Fig. 4. Accordingly, tan δ variation is: PCH_{105}-*b*-P*i*BA_{355}-*b*-PCH_{105} < PCH_{219}-*b*-P*i*BA_{355}-*b*-PCH_{219} < PCH_{299}-*b*-P*i*BA_{355}-*b*-PCH_{299} ≈ PCH_{380}-*b*-P*i*BA_{355}-*b*-PCH_{380} because the molecular cause of this relaxation is ascribed to the cyclohexyl groups. On the contrary of the γ^{PiBA} process the location and apparent activation energy are dependent on outer block molecular weight. Thus, the relaxation is shifted to higher temperatures and activation energy is slightly increased as PCH length is raised in the copolymer.

However, the effect of composition on the intensity is much more significant in those relaxations associated with the glass transition of the inner and outer blocks, α^{PiBA} and α^{PCH}, respectively. Therefore, in PCH_{105}-*b*-P*i*BA_{355}-*b*-PCH_{105} the α^{PiBA} intensity is the highest and that related to the α^{PCH} the smallest. Little differences are found in the other three block copolymers. Other feature is that small amounts of PCH as outer blocks considerably shift the α^{PiBA} mechanism at higher temperatures indicating a mobility hindrance and the α^{PCH} process at lowest temperatures pointing out that generalized motion within the PCH block is favored as PCH length is short enough. These characteristics might be related to the arrangements of both blocks. Although phase separation exists, as the presence of two glass transition temperatures determined by DSC, WAXS and DMTA indicates, it seems that the PCH blocks are too short in the copolymer with the highest P*i*BA composition ratio that none of the ordering between these two types of existing segments can be developed, as will be commented in Section 3.2 through the SAXS and AFM results. Concerning the α^{PiBA} relaxation for the other PCH_X-*b*-P*i*BA_{355}-*b*-PCH_X copolymers, its location is moved slightly

Table 2
Relaxation temperatures (on tan δ basis at 3 Hz) and apparent activation energy for the different relaxation processes in the PCH_X-*b*-P*i*BA_{355}-*b*-PCH_X block copolymers under tensile deformation

Sample	*T* (°C)					Δ*H* (kJ mol^{-1})				
	γ^{PiBA}	γ^{PCH}	α^{PiBA}	β^{PCH}	α^{PCH}	γ^{PiBA}	γ^{PCH}	α^{PiBA}	β^{PCH}	α^{PCH}
PCH_{105}-*b*-P*i*BA_{355}-*b*-PCH_{105}	−147.5	−75.5	−2.0	27.5	115.0	40	50	210	75	220
PCH_{219}-*b*-P*i*BA_{355}-*b*-PCH_{219}	−148.0	−74.5	−22.0	30.0	131.5	40	50	225	77	230
PCH_{299}-*b*-P*i*BA_{355}-*b*-PCH_{299}	−149.0	−67.0	−15.5	35.0	131.0	40	55	280	80	245
PCH_{380}-*b*-P*i*BA_{355}-*b*-PCH_{380}	−149.5	−65.0	−10.0	35.0	129.5	40	55	285	80	250

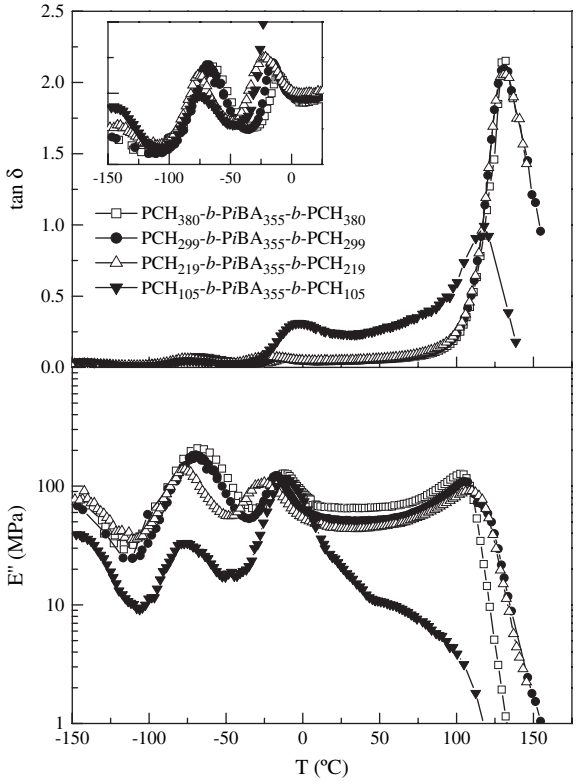

Fig. 4. Temperature dependence of loss modulus and loss tangent for the PCH_X-*b*-P*i*BA_{355}-*b*-PCH_X copolymers.

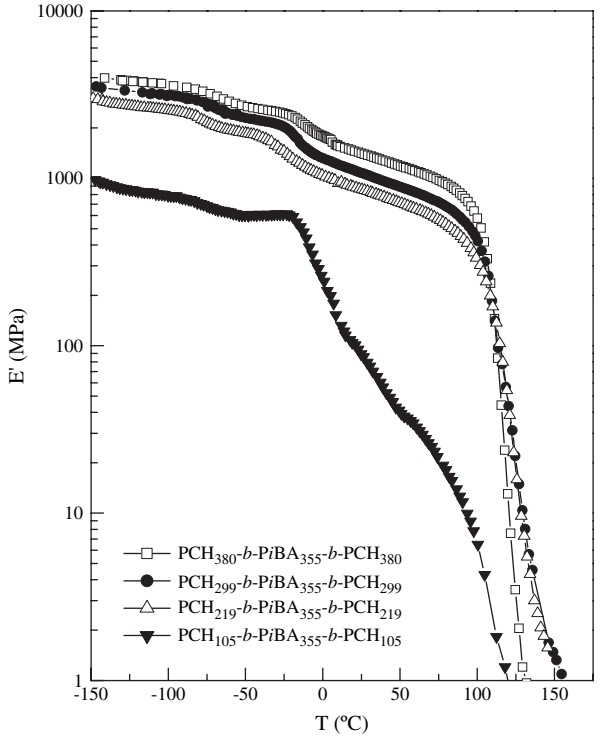

Fig. 5. Temperature dependence of storage modulus for the PCH_X-*b*-P*t*BA_{355}-*b*-PCH_X copolymers.

at higher temperature as PCH molecular weight increases whereas the position of α^{PCH} remains practically unchanged. In relation to the apparent activation energy of both cooperative relaxations, an increase of their values is observed as PCH length of outer blocks is raised in the copolymers.

Fig. 5 depicts the significant effect that composition has on the value of complex modulus elastic contribution. Accordingly, E' decreases as the stiffer PCH segment content does, the variation being quite considerable for the PCH_{105}-*b*-P*i*BA_{355}-*b*-PCH_{105} copolymer. The cyclohexyl groups provide rigidity to the inner and soft block as much as their content increases. In addition, the different relaxations can be observed in the E' representation. When a process occurs, a drop higher than that corresponding to the thermal expansion of the material takes places. Moreover, the magnitude of this drop is higher as the intensity of a given relaxation increases. Therefore, cooperative motions within each segments imply a significant diminution of rigidity and, thus, the E' reduction is much significant.

Fig. 6 shows the variation of microhardness with the PCH composition in the different copolymers. A significant increase is observed as content of stiff CH groups is raised in the copolymers. MH measures primarily the resistance of the material to plastic deformation and, accordingly, provides an idea about local strain. Several effects can be distinguished along microhardness measurements in semicrystalline polymers [36]: an elastic deformation that yields an instant elastic recovery on unloading; a permanent plastic deformation determined by arrangement and structure of crystallites and their connection by tie molecules and entanglements; and a time-dependent MH during loading and a long delayed recovery after load removal (viscoelastic contribution). Accordingly, MH estimation in temperature-variable measurements is

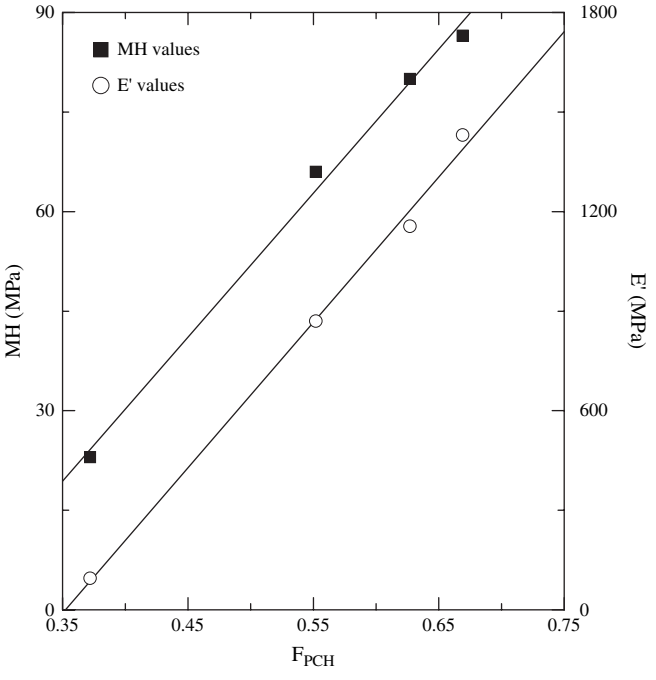

Fig. 6. Variation of microhardness and storage modulus values at 23 °C as a function of the poly(cyclohexyl methacrylate) content.

rather sensitive to all the parameters that change the mobility within the macromolecules. For instance, they have been used to estimate the glass transition temperature of the softer component in a set of microphase-separated graft copolymers [41].

Moreover, the dependence of E' value at 23 °C on PCH content is also represented in Fig. 6. An analogous trend is seen for both mechanical magnitudes. Although MH measurements are related to the superficial mechanical response, they also involve a complex combination of other bulk mechanical properties (elastic modulus, yield strength, strain hardening, toughness). A direct relationship is commonly found between the elasticity modulus and MH and the following empirical equation has been proposed [36]:

$$\mathrm{MH} = aE^b \tag{2}$$

where a and b are constants. This equation is also fulfilled by many amorphous and semicrystalline polymeric systems [40,41,48] in a very broad range of MH and E values: from thermoplastic elastomers to very rigid polymers. A good linear relationship in the log–log scale is also found in these block copolymers under study as depicted in Fig. 7.

3.2. Morphological arrangements

The existence of separated PCH and P*i*BA microphases has been confirmed by WAXS and DMTA measurements in agreement with DSC results [33]. However, these developed microdomains can be randomly distributed or, in other cases, may form a regular arrangement giving rise to a periodic structure [49] that usually generates profiles in the small angle X-ray region. Therefore, the SAXS profile analysis allows, if electron density contrast is high enough, identifying the morphology developed. Fig. 8 shows real-time temperature-variable heating–cooling profiles for the PCH_{380}-*b*-P*i*BA_{355}-*b*-PCH_{380} copolymer. These SAXS patterns are rather similar to those exhibited by the PCH_{299}-*b*-P*i*BA_{355}-*b*-PCH_{299} and PCH_{219}-*b*-P*i*BA_{355}-*b*-PCH_{219} copolymers. However, the block copolymer with the smallest PCH content does not show any maximum in the SAXS region. As previously commented, the length of the PCH blocks is too short and a partial miscibility with the inner segments seems to be obtained for this copolymer. On the other hand, the scattering vector, q, is defined as

$$q = \frac{4\pi \sin\theta}{\lambda}$$

and 2θ is the scattering angle and λ is the wavelength.

A unique peak is exclusively observed in Fig. 8 along the whole temperature range analyzed during heating and cooling processes. This fact seems to indicate the non-existence of an efficiently ordered arrangement in these copolymers prepared under the current experimental conditions. The lack of higher order reflections might point out that the electron density difference between the inner and outer blocks is too small, as occurred in other ABA (meth)acrylic block copolymers [34], or that there is not a microdomain ordering at long range. Looking at closely the diffraction peak, an increase of its intensity with temperature is seen for the heating process. In addition, a shift to lower q values, i.e. longer spacing is also observed. Moreover, width of this peak diminishes from 20 to 90 °C, remains practically unchanged ranged 90–130 °C and at higher temperatures significantly increases. All these features might be related to an improvement with increasing temperatures of the ordering between the existing PCH and P*i*BA microdomains. The position and width of the peak remain almost constant during the subsequent cooling.

The absence of the higher orders does not provide information about the specific morphology developed, although consistently with the copolymer composition of these PCH_X-*b*-P*i*BA_{355}-*b*-PCH_X copolymers a lamellar arrangement should be predicted. To elucidate this point, Fig. 9 shows an AFM picture for PCH_{380}-*b*-P*i*BA_{355}-*b*-PCH_{380} copolymer. In sharp contrast, the phase image is highly textured and consists of a complex pattern of bright and dark elongated objects. This pattern seems to point out the existence of an interpenetrated assembly of PCH and P*i*BA lamellae. The brighter areas that correspond to larger phase values are typical of component with higher modulus, i.e. PCH, whereas the darker ones are the signature of the softer component, the P*i*BA in the current block copolymers. These results seem to indicate that these block copolymers, with the exception of PCH_{105}-*b*-P*i*BA_{355}-*b*-PCH_{105}, exhibit a defective lamellar arrangement, whose Bragg spacing increases as outer PCH blocks molecular weight does, ranging its value from around 38 to 42 nm.

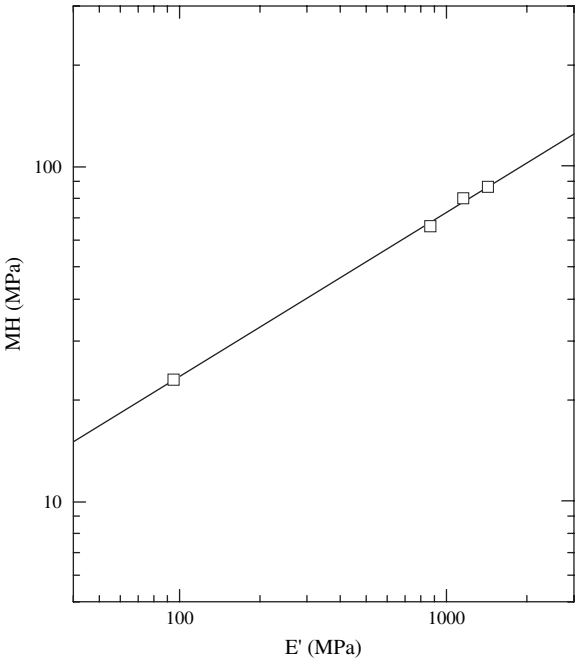

Fig. 7. Double-logarithmic relationships between MH and E' for the different PCH_X-*b*-P*t*BA_{355}-*b*-PCH_X specimens.

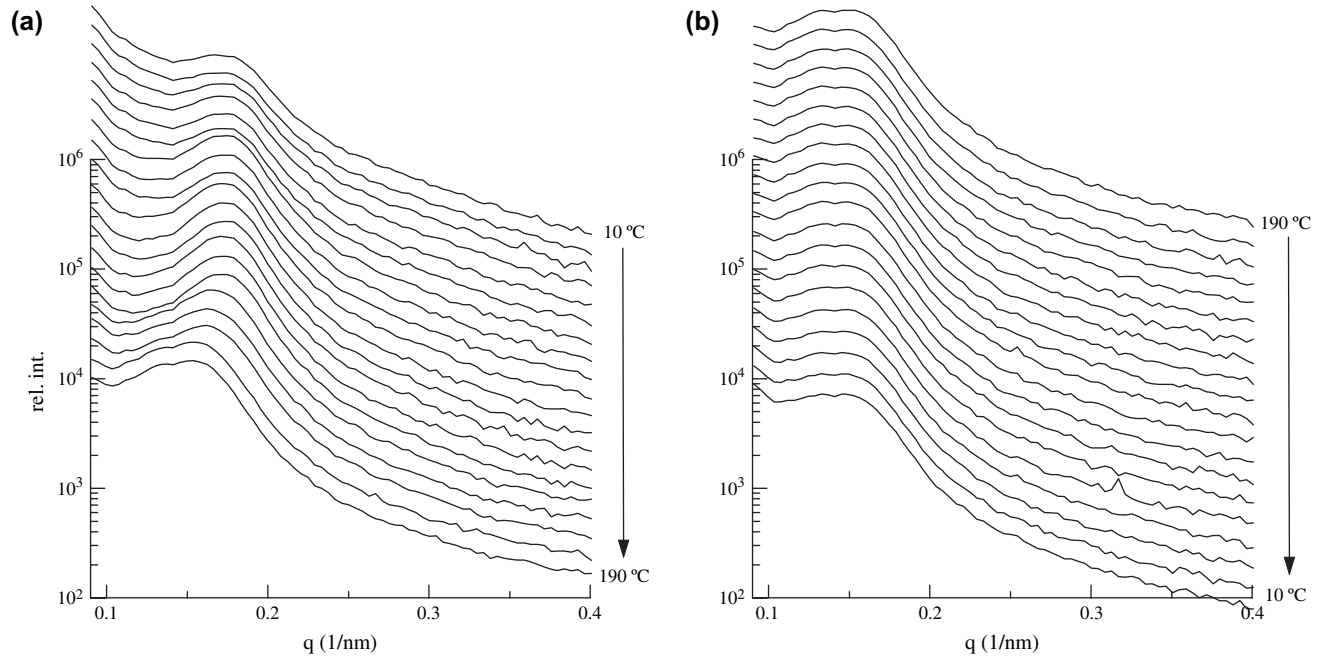

Fig. 8. Time-resolved SAXS profiles of PCH_{380}-*b*-P*i*BA_{355}-*b*-PCH_{380} triblock copolymer as a function of scattering vector: (a) first heating and (b) cooling processes.

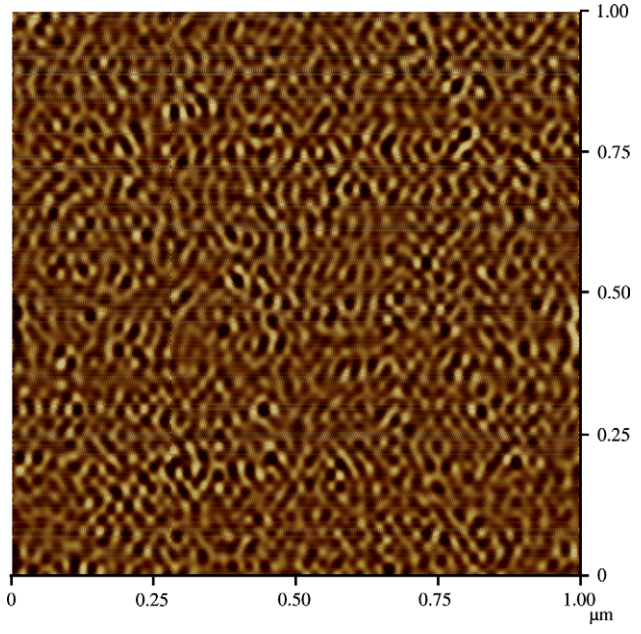

Fig. 9. AFM image for PCH_{380}-*b*-P*i*BA_{355}-*b*-PCH_{380} triblock copolymer.

4. Conclusions

The existence of microphase separation has been confirmed from WAXS profiles and from the presence and location of two relaxation processes associated with cooperative and generalized motions concerning each existing block in several PCH-*b*-P*i*BA-*b*-PCH triblock copolymers synthesized by atom transfer radical polymerization in a sequential manner. Moreover, other secondary relaxations have been found. Their intensities, positions and, sometimes, apparent activation energies are dependent on length of outer and hard PCH blocks.

The stiffness of these block copolymers has been also evaluated. On one hand, the values of E' decrease in the whole temperature range analyzed as the hard PCH segment content does, the diminishment being quite significant for the PCH_{105}-*b*-P*i*BA_{355}-*b*-PCH_{105} copolymer. On the other hand, the microhardness at room temperature increases as molecular weight of the PCH segments is raised, because it provides rigidity to the inner and soft P*i*BA block as much as their content increases. A linear relationship between E' and MH has been found at room temperature for these PCH_X-*b*-P*i*BA_{355}-*b*-PCH_X copolymers.

SAXS and AFM measurements seem to indicate that an interpenetrated assembly of PCH and P*i*BA lamellae without an ordering at long range is developed, with the exception of PCH_{105}-*b*-P*i*BA_{355}-*b*-PCH_{105} because of the short length of its PCH blocks.

Acknowledgment

The authors are grateful for the financial support of Ministerio de Educación y Ciencia (MAT2004-00496). The synchrotron work was supported by the European Community – Research Infrastructure Action under the FP6 ''Structuring the European Research Area'' Programme (through the Integrated Infrastructure Initiative ''Integrating Activity on Synchrotron and Free Electron Laser Science''), contract RII3-CT-2004-506008 (IA-SFS). We thank the collaboration of the Hasylab personnel in the soft-condensed matter beamline A2, especially Mr. M. Dommach and Dr. S. S. Funari.

References

[1] Wang JS, Matyjaszewski K. Macromolecules 1995;28:7901.
[2] Percec V, Barboiu B. Macromolecules 1995;28:7970.
[3] Kato M, Kamigaito M, Sawamoto M, Higashimura T. Macromolecules 1995;28:1721.
[4] Shipp DA, Wang JL, Matyjaszewski K. Macromolecules 1998;31:8005.
[5] Hamley IW. Block copolymers. Oxford, England: Oxford University Press; 1999.
[6] Hadjichristidis N, Pispas S, Floudas GA. Block copolymers. Synthetic strategies, physical properties and applications. New Jersey: John Wiley & Sons, Inc.; 2003.
[7] Hamley I. Developments in block copolymer science and technology. The Atrium, Southern Gate, Chichester, West Sussex, England: John Wiley & Sons, Inc.; 2004.
[8] Gowrishankar V, Miller N, McGehee MD, Misner MJ, Ryu DY, Russell TP, et al. Thin Solid Films 2006;513:289.
[9] Hempenius MA, Korczagin I, Vancso GJ. Metal-containing and metallo-supramolecular polymers and materials. ACS Sym Ser 2006;928:320.
[10] Yamaguchi T, Yamaguchi H. J Photopolym Sci Technol 2006;19:385.
[11] Tsige M, Mattsson TR, Grest GS. Macromolecules 2004;37:9132.
[12] Matyjaszewski K, Shipp DA, Mcmutry GP, Gaynor SG, Pakula T. J Polym Sci Part A Polym Chem 2000;38:2023.
[13] Tong JD, Moineau G, Ph Leclère, Brédas JL, Lazzaroni R, Jérôme R. Macromolecules 2000;33:470.
[14] Moineau G, Minet M, Dubois Ph, Teyssié Ph, Senninger T, Jérôme R. Macromolecules 1999;32:27.
[15] Moineau G, Minet M, Teyssié Ph, Jérôme R. Macromol Chem Phys 2000;201:1108.
[16] Moineau G, Minet M, Teyssié Ph, Jérôme R. Macromolecules 1999;32:8277.
[17] Uegaki H, Kotani Y, Kamigaito M, Sawamoto M. Macromolecules 1998;31:6756.
[18] Davis KA, Matyjaszewski K. Macromolecules 2000;33:4039.
[19] Davis KA, Matyjaszewski K. Macromolecules 2001;34:2101.
[20] Kamigaito M, Ando T, Sawamoto M. Chem Rev 2001;101:3689.
[21] Matyjaszweski K, Xia J. Chem Rev 2001;101:2921.
[22] Fernández-García M, de la Fuente JL, Fernández-Sanz M, Madruga EL. Polymer 2001;42:9405.
[23] Martín-Gomis L, Fernández-García M, de la Fuente JL, Madruga EL, Cerrada ML. Macromol Chem Phys 2003;204:2007.
[24] Masar B, Janata M, Vlcek P, Toman L, Kurkova D. J Appl Polym Sci 2002;86:2930.
[25] Masar B, Janata M, Vlcek P, Policka P, Toman L. Macromol Symp 2002;183:139.
[26] Darcos V, Haddleton DM. Eur Polym J 2003;39:855.
[27] Ramakrishnan A, Dhamodharan R. Macromolecules 2003;36:1039.
[28] Tsolakis PK, Kallitsis JK. Chem—Eur J 2003;9:936.
[29] Ning FL, Jiang M, Mu MF, Duan HW, Xie JW. J Polym Sci Polym Chem 2002;40:1253.
[30] Karanam S, Goossens H, Klumperman B, Lemstra P. Macromolecules 2003;36:3051.
[31] Qin SH, Saget J, Pyun JR, Jia SJ, Kowalewski T, Matyjaszewski K. Macromolecules 2003;36:8969.
[32] Karakatsanis E, Focke W, Summers G. Macromol Symp 2003;193:187.
[33] Muñoz-Bonilla A, Cerrada ML, Fernández-García M. J Polym Sci Part A Polym Chem 2005;43:4828.
[34] Tong JD, Leclère Ph, Doneaux C, Brédas JL, Lazzaroni R, Jérôme R. Polymer 2001;42:3503.
[35] McCrum NG, Read BE, Williams G. Anelastic and dielectric effects in solid polymers. New York: Dover; 1991.
[36] Baltá-Calleja FJ. Adv Polym Sci 1985;66:117.
[37] Klug HP, Alexander LE, editors. X-ray diffraction procedures for polycrystalline and amorphous materials. New York: Wiley; 1954. p. 632.
[38] Nielsen LE, Landel RF. Mechanical properties of polymers and composites. 2nd ed. New York: Marcel Dekker Inc.; 1994.
[39] Menissez C, Sixou B, David L, Vigier C. J Non-Cryst Solids 2005;351:595.
[40] Cerrada ML, de la Fuente JL, Fernández-García M, Madruga EL. Polymer 2001;42:4647.
[41] Cerrada ML, de la Fuente JL, Madruga EL, Fernández-García M. Polymer 2002;43:2803.
[42] Díaz-Calleja R, Sanchis MJ, Álvarez C, Riande E. J Appl Phys 1996;80:1047.
[43] Saiz E, Riande E. J Chem Phys 1995;103:3832.
[44] Ribes-Greus A, Gómez-Ribelles JL, Díaz-Calleja R. Polymer 1985;26:1849.
[45] Fytas G. Macromolecules 1989;22:211.
[46] Rotter G, Ishida H. Macromolecules 1992;25:2170.
[47] Mark HF, Bikales NM, Overberger CG, Menges G. Encyclopedia of polymer science and engineering. 2nd ed., vol. 16. New York: Wiley-Interscience Publication, John Wiley and Sons; 1989.
[48] Cerrada ML, Benavente R, Pérez E, Moniz-Santos J, Ribeiro MR. J Polym Sci Part B Polym Phys 2004;42:3797.
[49] Kim WG, Garetz BA, Newstein MC, Balsara NP. J Polym Sci Part B Polym Phys 2001;39:2231.